RELATIONSHIPS BETWEEN NON-WETTING PHASE INVASION AND MAGNETIZATION EVOLUTION IN CONNECTED PORE SYSTEMS AS REVEALED BY NETWORK SIMULATION

D. Chang, M.A. Ioannidis and I. Chatzis
Porous Media Research Institute
Department of Chemical Engineering
University of Waterloo

ABSTRACT

Pore network models are used to relate fundamental pore structure parameters (pore body and pore throat size distributions) to the distribution of water at the pore level and the decay of proton magnetization under conditions of primary drainage in water-wet rocks. The simulations reveal conditions under which diffusive coupling between pores has a significant effect on the decay spectra and provide insight into the estimation of primary drainage capillary pressure curves from NMR T_2 distributions. The conversion factor $k = P_c\ T_2$ required to map a NMR cumulative T_2 distribution at S_w = 100% onto a primary drainage capillary pressure curve furnishes important information about the pore-to-throat size aspect ratio, a parameter that critically affects recovery efficiency by waterflooding in water-wet media.

INTRODUCTION

With the advent of NMR wireline logging tools, the feasibility of estimating primary drainage capillary pressure curves from the NMR T_2 distributions of water-saturated rock samples has recently attracted significant attention (*e.g.*, Volokitin *et al.*, 1999). In a NMR measurement, hydrogen atoms on water molecules probe the pore space by diffusive motion. The magnetic moment carried by these atoms relaxes due to dipolar interactions with other molecules and with the fluid-solid interface. For a single pore in the fast diffusion limit, the surface relaxation rate is slow compared to the rate of magnetization equilibration by diffusive motion (Brownstein and Tarr, 1979). Consequently, magnetization is approximately uniform across the pore and decays with a characteristic time T_2 that is inversely proportional to the pore's surface area-to-volume ratio:

$$\frac{1}{T_2} = \rho \frac{A}{V} \tag{1}$$

The proportionality constant ρ is known as the surface relaxivity and knowledge of its value allows one to convert a rate of surface relaxation to a characteristic pore size R_p (*e.g.*, $A/V = 3/R_p$ for spherical pores). The time evolution of proton magnetization in sedimentary rocks is usually characterized by a spectrum of decay rates (Kenyon, 1997), a fact used to estimate the distribution of pore volume by pore size. Such estimates are invariably made under the assumption that, although in the fast diffusion limit, individual pores are uncoupled from their neighbors. The effect of this assumption has been theoretically investigated by McCall *et al.* (1991). These authors studied network models in which the sizes of pores were broadly distributed, but the pore throat cross-sectional areas and inter-pore diffusion lengths were assumed constant. Such models are not quite representative of the pore structure of reservoir rocks, in which pore throats are known to also be broadly distributed. This is borne out by observation of mercury intrusion curves of reservoir rock samples, which show significant penetration over a wide range of capillary pressures. Nonetheless, McCall *et al.* (1991) suggested that in a system with a broad distribution of pore sizes, in the range typically found in sandstones, pore coupling should be marginally significant. This implies that the spectrum of decay rates obtained by multi-exponential decomposition of total magnetization measurements should reflect the volume density of pore sizes reasonably well. In the limit of "strong enough" diffusive coupling between pores, the entire pore space would behave as a single pore in the fast diffusion limit and the spectrum of decay rates would be a δ-function centered at $\rho A/V$, where A and V are the total area and pore volume. What constitutes "strong enough" coupling and how it affects the magnetization decay spectra, especially of partially-saturated porous media, is still not fully understood.

A primary drainage capillary pressure curve provides the distribution of pore volume accessible to a non-wetting phase by capillary pressure. The latter is related to the size of pore throats that are accessible to a non-wetting phase during drainage through the Laplace equation:

$$P_c = \frac{\sigma f(\theta)}{R_t} \tag{2}$$

where R_t is a characteristic pore throat size and $f(\theta)$ is a function of the mercury-air advancing contact angle that depends on the geometry of the pore throat cross-section (*e.g.*, $f(\theta) = 2\cos\theta$ for cylindrical pore throats).

Even if a NMR T_2 distribution adequately reflects the distribution of pore volume by pore size (*i.e.*, if diffusive coupling effects are insignificant), additional assumptions are necessary to convert this distribution into a drainage capillary pressure curve. Namely, it is necessary to assume that (i) the pore-body to pore-throat size aspect ratio is either constant or known as a function of pore body size, (ii) that non-wetting phase invasion into a pore network is not subject to accessibility constraints and (iii) that, upon invasion by a non-wetting phase, pores are fully drained. Assumption (ii) ignores the fact that

some large pores are invaded at capillary pressures higher than the pressures corresponding to the size of pore throats they are connected to, because they are "shielded" by smaller pores. Assumption (iii) ignores the fact that, upon invasion by the non-wetting phase into a pore, pore corners and roughness features remain occupied by the wetting phase. Thus, only a fraction of the volume of each pore probed by water molecules during a NMR experiment is also probed by a non-wetting phase when the pore is first invaded. The purpose of this paper is to examine the impact of these phenomena on decay rate spectra by means of computer simulation in model pore networks. Pore networks with prescribed pore and throat size distributions and pore coordination number are constructed and primary drainage by a non-wetting phase is simulated using a bond-correlated site percolation algorithm.

NETWORK SIMULATION APPROACH

Construction of model pore networks

The pore structure model used is similar to the one used by Ioannidis and Chatzis (1993) to simulate the permeability, formation factor and drainage capillary pressure curves of several sandstones. It is a simple cubic network of pores and throats of square cross-section (Fig. 1). Pore body sizes are randomly assigned to the sites of the network, whereas pore throat sizes are correlated to the size of the smaller of the two pores each throat connects. Pore body and pore throat sizes are assumed to follow respective shifted Weibull distribution functions (Shapiro and Gross, 1981). These distributions were used for their versatility:

$$\mathrm{f_i(R)} = \left(\frac{b}{a}\right)\cdot\left(\frac{\mathrm{R}-\mathrm{R_{min}}}{a}\right)^{b-1}\cdot\exp\left[-\left(\frac{\mathrm{R}-\mathrm{R_{min}}}{a}\right)^{b}\right] \qquad \begin{array}{l} i = p,b \\ p = pores \\ t = throats \end{array} \qquad (3)$$

where a, b are parameters of the distributions and $R_{\min}$ is a minimum pore body or pore throat size. Fixing the porosity of the network determines the distance between pores, thus permitting the estimation of pore throat lengths, L_{ij}. These lengths are only used to estimate the resistance to diffusion and fluid flow between adjacent pores; all pore volume is assigned to the pore bodies. Network models containing 15^3 pore bodies are used throughout this work. All results reported are averages over 10 realizations.

Simulation of magnetization evolution in model pore networks

A balance of magnetization M_i may be written for each pore i in the network. The net rate of magnetization decay in each pore is determined by magnetization relaxation in the vicinity of the fluid-matrix interface and by diffusion to and from neighboring pores:

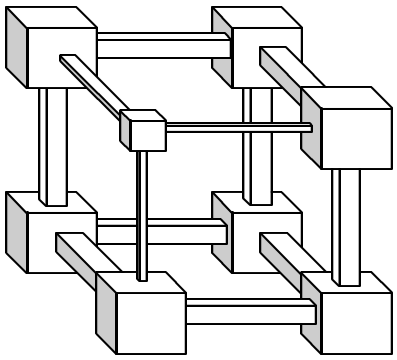

Figure 1. Schematic representation of the geometry of the pore network model.

$$\frac{dM_i}{dt} = -r \cdot A_i \cdot \frac{M_i}{V_i} + D \cdot \sum_j^{NN} \frac{S_{ij}}{L_{ij}} \cdot \left(\frac{M_j}{V_j} - \frac{M_i}{V_i} \right) \tag{4}$$

where A_i, V_i are the surface area and volume of pore i, respectively, D is the diffusion coefficient of water and S_{ij}, L_{ij} are the cross-sectional area and length of connecting pore throats. In dimensionless form, Eq. (4) may be written as follows:

$$\frac{dM_i}{dt} = -w_r \cdot r_i \cdot M_i + w_c \cdot \sum_j^{NN} \frac{s_{ij}}{l_{ij}} \cdot \left(\frac{M_j}{v_j} - \frac{M_i}{v_i} \right) \tag{5}$$

In writing Eq. (5) the following definitions are used:

$$w_r = r \times \frac{\overline{A}}{\overline{V}} = \frac{1}{t_o} \qquad w_c = \frac{D\overline{S}}{\overline{V}\,\overline{L}}$$

$$s_{ij} = \frac{S_{ij}}{\overline{S}} \qquad l_{ij} = \frac{L_{ij}}{\overline{L}} \tag{6}$$

$$v_{ij} = \frac{V_{ij}}{\overline{V}} \qquad r_i = \frac{A_i}{V_i} \times \frac{\overline{V}}{\overline{A}}$$

In the equations above, overbars indicate average quantities. The parameters w_r and w_c represent a characteristic rate of relaxation at the fluid-solid interface and a characteristic rate of molecular diffusion between pores, respectively. Application of Eq. (5) to each pore yields an initial-value, linear ordinary differential equation problem, which is most

efficiently solved by matrix diagonalization methods (McCall *et al*., 1991). The solution provides the volume-weighted distribution $n(\lambda)$ of decay rates λ, hereafter referred to as sprectrum of decay rates, where each λ is an eigenvalue of the problem. In the absence of coupling between pores, $\lambda_i = \rho A_i / V_i$ and the spectrum $n(\lambda)$ exactly corresponds to the distribution of pore volume by inverse pore size.

Simulation of primary drainage

Simulation of primary drainage is carried out using a bond-correlated site percolation algorithm described in detail by Ioannidis and Chatzis (1993). It is assumed in the simulations that, once a pore is invaded by the non-wetting phase, a fraction equal to 6% of its volume V_i remains occupied by water. This residual water is also assumed to have access to the entire surface area A_i of the pore. Water diffusion between neighboring pores that are both invaded by the non-wetting phase is assumed to take place through constrictions whose cross-sectional area is 6% of the cross-sectional area S_{ij} of the connecting pore throat. This value corresponds to the water saturation in capillaries of square cross-section at conditions of gas breakthrough (Legait, 1983). Of course, a more realistic treatment of "late pore-filling" may involve other assumptions on the geometry of corners and crevices and should provide residual water saturation values that decrease with increasing capillary pressure in each invaded pore.

RESULTS AND DISCUSSION

Porous media properties

We have considered two rather different pore network models, hereafter referred to as Model 1 and Model 2. Their respective pore body size distributions (PSD) and pore throat size distributions (TSD) are shown in Fig. 2. Model 1 corresponds to a medium with a rather uniform TSD that significantly overlaps the PSD and is more typical of unconsolidated materials. Model 2 corresponds to a medium with a heavily skewed TSD and is more typical of reservoir sandstones (Ioannidis and Chatzis, 1993a).

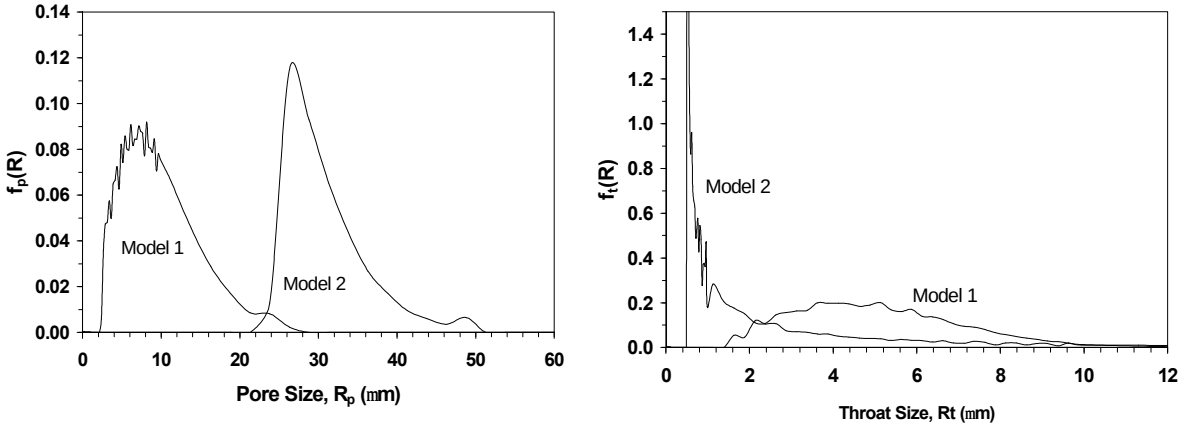

Figure 2. Pore body and pore throat size distributions used in network simulations

Note that the throat size distribution for Model 2 is not completely shown in Fig.2 because there is a long tail to a maximum throat size of 94 μm and it truly has a mean throat size equal to 4 μm. Table 1 lists relevant simulation parameters, including the computed absolute permeability of each model. A value of surface relaxivity typical of sandstones (100 μm/s) is used in all computations (Slijkerman and Hofman, 1998; Roberts *et al*., 1995).

Table 1: Pore network model characteristics and simulation parameters

Parameter	*Model 1*	*Model 2*
Mean of PSD (μm)	10	31
Standard deviation of PSD (μm)	5	5
Minimum pore size (μm)	2	25
Maximum pore size (μm)	26.3	98.8
Mean of TSD (μm)	5	4
Standard deviation of TSD (μm)	2	7
Minimum throat size (μm)	1	0.5
Maximum throat size (μm)	13.8	93.8
Porosity (%)	17.8	17.8
Permeability (mD)	459	32.5
Water Diffusivity ($\mu m^2/s$)	2500	2500

Decay of proton magnetization during primary drainage

Knowledge of the water distribution at the pore level, obtained by simulation of primary drainage, enables determination of the magnetization decay spectra at different values of water saturation. Pore coupling is insignificant at all saturation levels in Model 2. This is mainly due to the higher frequency of small throat sizes in this model, which result in a much higher diffusion resistance in the network. Decay spectra at various levels of water saturation in this system are shown in Fig. 3. The spectrum at S_w = 100% reflects the narrow distribution of pore sizes in this system. Primary drainage results in gradual disappearance of slow decay rates from the spectrum as water is being drained from the larger pores. Further reduction of S_w causes the appearance of fast rates in the spectrum, associated with the presence of residual water in the pore corners, which are not present in the spectrum at S_w = 100%. Unlike Model 2, the effects of diffusive pore coupling in Model 1 are evident at all saturation levels. As shown in Fig. 4(a), diffusion between pores at S_w = 100% narrows the spectrum of decay rates and skews it towards larger rates. The effect of coupling is more pronounced at lower levels of water saturation, as shown in Fig. 4(b). The evolution of decay spectra with S_w is illustrated in Fig. 5. As with

Model 2, accounting for the presence of residual water in pores invaded by the non-wetting phase significantly extends the spectrum of decay rates at low S_w.

Drainage capillary pressure curves from T_2 distributions

In order to convert a NMR T_2 distribution at S_w = 100% to a primary drainage capillary pressure curve, Volokitin *et al.* (1999) suggested the use of a variable $k = P_c/l$ scaling factor, namely one that increases with increasing P_c. The network modeling approach pursued in this study allows us to explore the nature of this conversion and determine the relationship of the scaling factor to the pore and throat size distributions. A variable scaling $k(P_c)$ suggested by Volokitin *et al*. (1999) is given below:

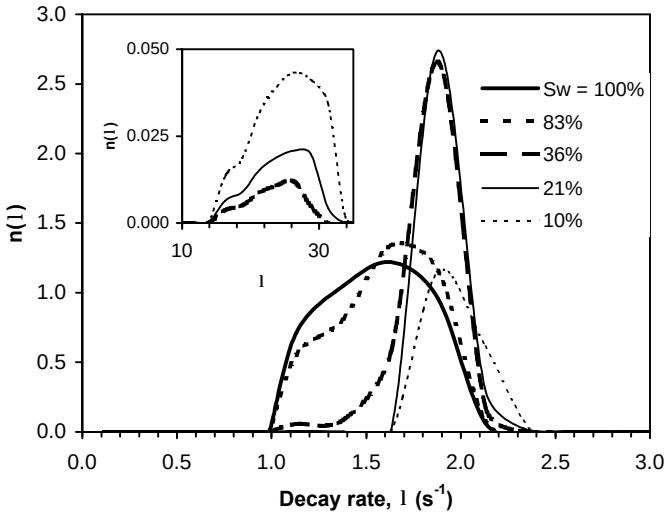

Figure 3. Magnetization decay spectra for Model 2 during primary drainage. Inset shows the fast-rate components of the spectra at low S_w.

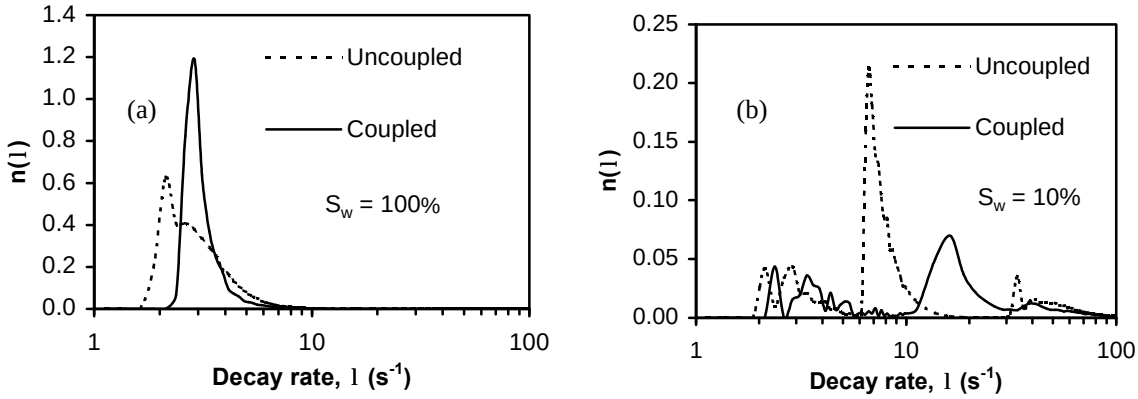

Figure 4. Effect of pore coupling on magnetization decay spectra of Model 1: (a) S_w = 100%, (b) S_w = 10%.

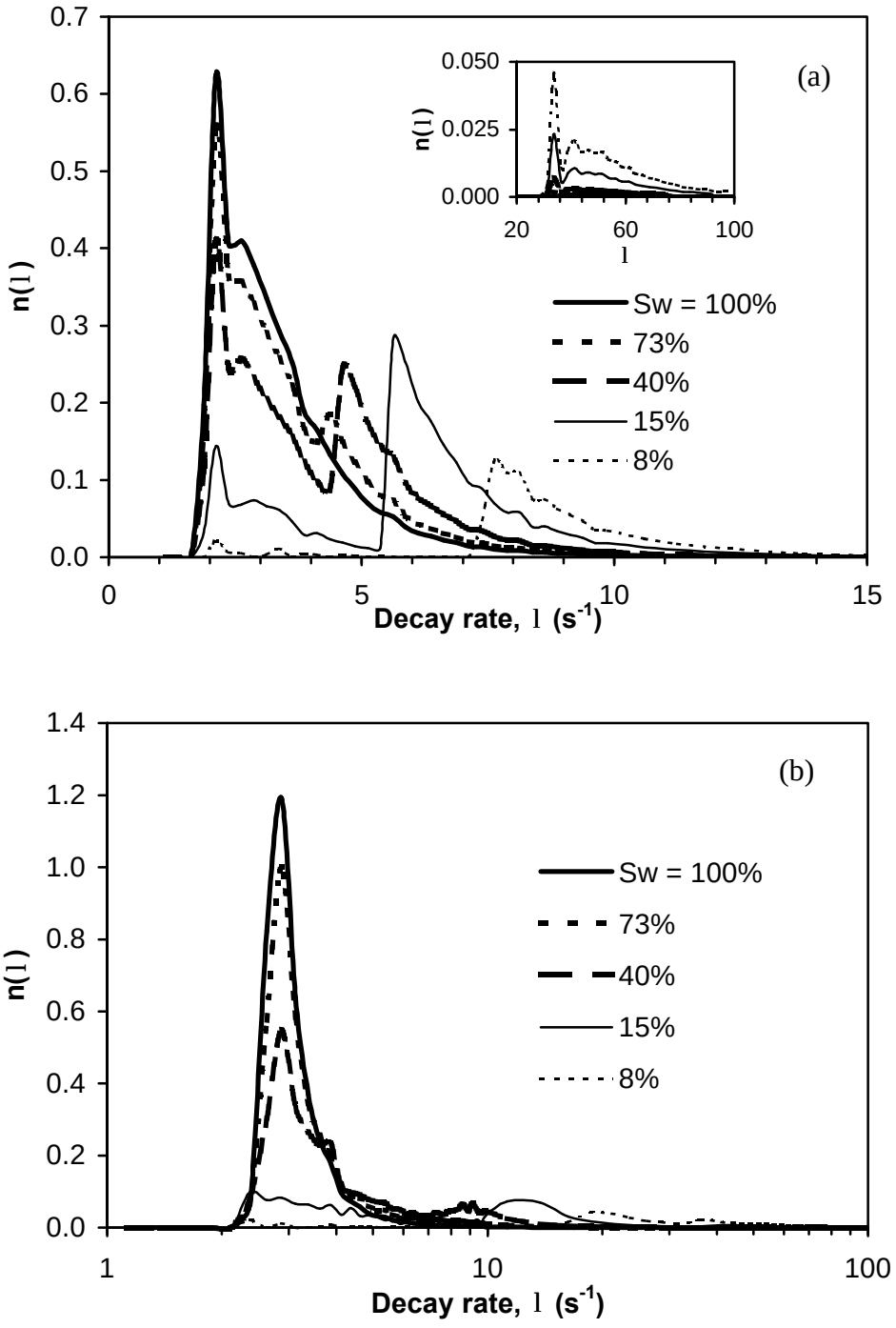

Figure 5. Magnetization decay spectra for Model 1 during primary drainage: (a) pore coupling ignored, (b) pore coupling accounted for.

$$k(P_c) = k_o \left[1 + \frac{A}{\left(B/P_c + 1\right)^C}\right] \tag{7}$$

where A,B,C and k_o are adjustable constants determined by optimization methods. If it can be assumed that the surface relaxivity is independent of pore size, then the value of k reflects an effective pore body-to-pore throat size aspect ratio.

The functions $k(P_c)$ of the form of Eq. (7) which best reproduce the drainage capillary pressure curves of Model 1 and Model 2 are shown in Fig. 6, whereas the simulated drainage capillary pressure curves and those obtained from the NMR T_2 distributions are compared in Fig. 7. A nearly constant scaling factor $k \approx 4.7$ is obtained for Model 1. This model has a rather uniform and relatively narrow TSD (see Fig. 2). Thus, primary drainage in this model takes place within a narrow range of capillary pressures, giving a rather steep drainage capillary pressure curve. Using the value of r for sandstone = 100 μm/s, we estimate a pore-to-throat size aspect ratio of 2.2 from $k \approx$ 4.7. This value is to be compared with the actual aspect ratio of the smallest pores and throats accessible at breakthrough conditions in Model 1 (P_c = 13.4 psi; S_w = 0.80), the latter value being equal to 1.5. Even though there is a difference in the magnetization decay spectra for Model 1 (having a pore structure with narrow throat size distribution), no significant difference was found for the κ values, as seen from the results show in Figure 6.

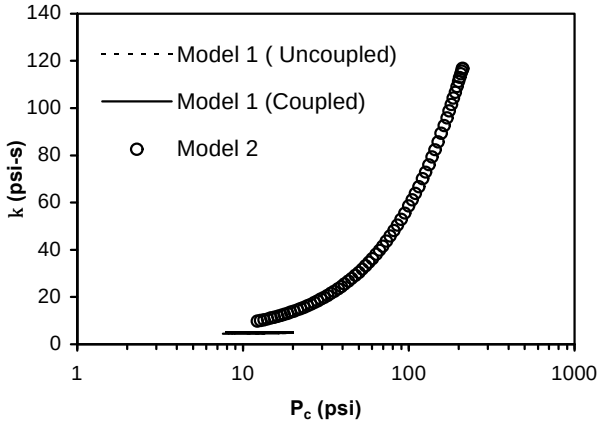

Figure 6. Scaling factor k used to convert NMR decay spectra to primary drainage capillary pressure curves. Data shown correspond to $0.10 < S_w < 0.80$ for Model 1 and $0.10 < S_w < 0.88$ for Model 2.

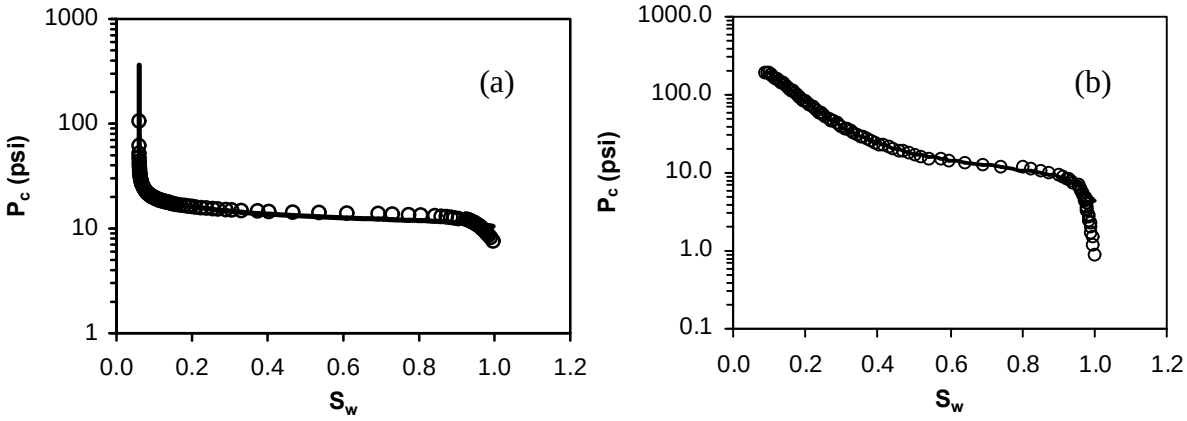

Figure 7. Simulated (points) and NMR-reconstructed (lines) primary drainage capillary pressure curves: (a) Model 1, (b) Model 2.

Model 2 is characterized by a broader TSD that is heavily skewed towards smaller pore throat pore throat sizes (see Fig. 2). This gives rise to a much more gradual capillary pressure curve that extends over a wider capillary pressure range. As shown in Fig. 6, the scaling factor k required to reproduce the capillary pressure curve from the NMR decay spectrum at S_w = 100% (Fig. 3) is not constant in this case. The aspect ratio of the smallest pores and throats accessible at breakthrough conditions in Model 2 (P_c = 11.3 psi; S_w = 0.88) is equal to 2.7. This value is to be compared with the aspect ratio of 4.3, estimated using κ(at P_c = 11.3 psi) = 9.3. An estimated higher aspect ratio is consistent with the pore and throat size distributions of this model (Fig. 2). However, the apparent aspect ratio calculated from the k values at breakthrough conditions is higher than the actual aspect ratio of the pores and throats involved. This discrepancy reflects the effect of limited pore accessibility near the percolation threshold. The results indicate that scaling NMR T_2 distributions to primary drainage capillary pressure curves provides information about an apparent pore body-to–pore throat size aspect ratio. This is an important pore structure parameter affecting the magnitude of residual non-wetting phase saturation after imbibition (Ioannidis and Chatzis, 1993b).

CONCLUSIONS

1. The NMR response of partially saturated porous media during drainage displacements, can be efficiently simulated using network models of pore structure with pore and throat size distributions. The same type of network models have been used in previous studies of our group to predict a host of petrophysical properties dependent on fluid distributions at the pore scale. In this paper, we provide a useful approach to relate NMR T_2 distributions from partially saturated porous media to drainage capillary pressure curves and corresponding fluid distributions.

2. In the fast diffusion limit, pore coupling can be significant in media with a broad pore size distribution when the throat size distribution and inter-pore length are taken into account. In such cases, pore coupling is more pronounced at lower wetting phase saturations.
3. For the cases studied, simulations confirm that the conversion of NMR T_2 distributions to primary drainage capillary pressure curves provides information about the size aspect ratio of pore throats and pore bodies, which may be usefully correlated to recovery efficiency.

NOMENCLATURE

T_2 – NMR relaxation time (s)
A_i – Surface area of pore i (μm^2)
V_i – Volume of pore i (μm^3)
S_{ij} – Cross sectional area of throat connecting pores i and j (μm^2)
L_{ij} – Diffusion length between pores i and j (μm)
R_p – Characteristic pore size (μm)
R_t – Characteristic throat size (μm)
R_{min} – Minimum pore or throat size (μm)
D – Diffusion coefficient ($\mu m^2/s$)
M_i – Normalized magnetization of pore i
S_w – Water saturation
P_c – Capillary pressure (psi)
α – Weibull location/spread parameter
β – Weibull kurtosis/skewness parameter
ρ – Surface relaxivity ($\mu m/s$)
σ – Surface tension (N/m)
ω_ρ – Characteristic rate of relaxation at the fluid-solid interface (1/s)
ω_c – Characteristic rate of molecular diffusion between pores (1/s)
λ – Relaxation rate (1/s)
κ – Scaling factor between λ and P_c (psi·s)

REFERENCES

Brownstein, K.R. and Tarr, C.E., "Importance of classical diffusion in NMR studies of water in biological cells", Physical Review A, (1979) 19, 2446-2453.

Ioannidis, M.A. and Chatzis, I., "Network modelling of pore structure and transport Properties of Porous Media", Chemical Engineering Science, (1993a) 48, no. 5, 951-972.

Ioannidis, M.A. and Chatzis, I., “A mixed-percolation model of capillary hysteresis and entrapment in mercury porosimetry”, Journal of Colloid and Interface Science, (1993b) 161, 278-291.

Kenyon, W.E., “Petrophysical principles of applications of NMR logging”, The Log Analyst, (1997) 38, no. 2, 21-43.

Legait, B., “Laminar flow of two phases through a capillary tube with variable square cross-section”, Journal of Colloid and Interface Science, (1983) 96, no. 1, 28.

McCall, K.R., Johnson, D.L. and Guyer, R.A., “Magnetization evolution in connected pore systems”, Physical Review B, (1991) 44, no. 14, 7344-7355.

Roberts, S.P., McDonald, P.J., and Pritchard, T., “A bulk and spatially resolved NMR relaxation study of sandstone rock plugs”, Journal of Magnetic Resonance, (1995) Series A 116, 189-195.

Shapiro, S.S. and Gross, A.J., “Statistical Modeling Techniques”, Marcel Dekker, New York, 1981.

Slijkerman, W.F.J., and Hofman, J.P., “Determination of Surface Relaxivity from NMR diffusion measurements”, Magnetic Resonance Imaging, (1998) 16, no. 5/6, 541-544.

Volokitin, Y., Looyestijn, W.J., Slijkerman, W.F.J. and Hofman, J.P., “A Practical Approach to Obtain 1st Drainage Capillary Pressure Curves from NMR Core and Log Data”, SCA-9924, 1999.